

Conceptual design of cost-effective ice detection system based on infrared thermography

Adeel Yousuf^{*}, Hassan Khawaja, Muhammad S. Virk

UiT-The Arctic University of Norway, Norway

ARTICLE INFO

Keywords:

Ice detection
Ice mitigation
Infrared thermography
Automation
System development

ABSTRACT

Ice accretion has been a persisting issue in cold regions and poses a threat to both onshore and offshore infrastructure, especially to sensitive equipment and personnel safety. Thermal infrared imaging (thermography) can be used as a non-destructive, non-invasive technique to determine the presence and thickness of ice over a surface. This paper presents early-stage experiment results with a FLIR® Lepton 2.5 radiometric thermal IR camera (resolution 80 × 60) to detect ice. Other technical aspects are also studied qualitatively, and corresponding results are validated against a high-speed, high-resolution FLIR® T1030SC thermal IR camera. The presented results are the first step in detecting and mitigating ice on flat surfaces. This technique may lead to the development of autonomous, remote, economical ice detection and mitigation system.

1. Introduction

Cold regions worldwide, specifically Arctic polar regions, are experiencing progressive logistic and infrastructure development both onshore and offshore due to technological advancement and growing competition for resources. However, such development is impeded by the harsh cold climatic conditions pertaining to ice accretion on structures, which drastically affects every related industry. In aviation, supercooled water droplets convert into ice upon surface impingement and change the aerodynamics of aircraft (Muhammed and Virk, 2022; Szilder and Yuan, 2017; Muhammed and Virk, 2023a). Rotorcrafts endure ice accretion on propellers and vital engine parts (Cao and Chen, 2016; Muhammed and Virk, 2023b). In railways, precipitation icing may cause flashovers and derailment and hence disruption to rolling stock (Network Rail, n.d.; Kandelin, 2021; Qi et al., 2022). Maritime activities and Search And Rescue (SAR) operations also get affected; lifeboats cannot be launched as the locks that attach them to the vessels get frozen (Virk et al., 2011). Atmospheric icing on the overhead powerlines and telecommunication cables leads to insulator flashover, sagging, and ice-shedding, incurring human life loss and property damage (Farzaneh, 2013; Farzaneh and Kiernic, 1995; Farzaneh and Melo, 1990; Hu et al., 2014). Onshore wind turbines' operation gets limited due to the ice accretion leading to ice-shedding. Icing-induced power losses in turbines may reach up to as high as 80% of all the incurred losses (Virk and Afzal, 2018). The situation becomes more rigorous for offshore wind

turbines, vessels, and platforms, such as oil rigs, as they get impacted by atmospheric icing and wave- and wind-induced sea spray icing (Hansen, 2012). Specialized drilling vessels and tools need to be designed for fossil-fuel extraction that can withstand harsh weather conditions (Ryerson, 2011).

In order to overcome icing hazards, ice mitigation systems are developed depending upon the application (aviation, railway, etc.). These include anti-icing procedures (like electrothermal, hot-air, pneumatic boots, microwave, coatings, chemical sprays, etc.) or de-icing techniques (like the creation of MAGnetic Slippery Surfaces – MAGSS, Electro Impulsive De-Icing – EIDI, Electro Expulsive De-Icing – EEDI, etc.) (Virk et al., 2011; Wei et al., 2019; Mustafa and Virk, 2011). However, before ice-mitigation systems work, an ice detection strategy needs to be devised for an autonomous operation. In this regard, some indirect methods usually based on statistical data analysis to predict icing potential are being used (Jin and Virk, 2019). The disadvantage is that met masts or sensors for this technique are established at far-off locations than the actual target location, so accuracy is a concern. An alternate is the direct measurement technique which includes vibration diaphragms, ultrasonic/microwave transducers, capacitive/inductive sensors, infrared probes, or temperature sensors. However, all of these are point-based sensors that measure a physical parameter affected by ice presence at a particular position and also require retrofitting over the target surface (Mustafa and Virk, 2011). Optical and Infra-Red Thermography (IRT), on the other hand, offer the characteristics of remote-

^{*} Corresponding author: UiT The Arctic University of Norway in Narvik, Lodve Langes gate 2, 8514 Narvik, Norway.
E-mail address: yousuf.adeel@uit.no (A. Yousuf).

sensing and area-based imagery. Optical technique based on true color, in some instances, confuses icing on the target surface (e.g., overhead power lines) with the background (e.g., icing on trees, white clouds) (Mustafa and Virk, 2011). (Active) Infrared thermography appears as a non-destructive, non-invasive technique that creates a contrast for the object to be segmented out of the imagery based on temperature variation.

2. Background

2.1. Image acquisition & processing

The output image captured by some typical high quality thermal infrared camera is basically a radiometric image with pixels representing recorded temperature in the form of 16-bit unsigned integer values (0–65,535). When observed as false-color image (3 channel RGB x 8bit) or simple 8-bit greyscale image, these values are mapped to 0–255. Processing the 8-bit greyscale images is equivalent to processing 24-bit false-color RGB in terms of contrast adjustment and edge-detection however former one is computationally less expensive (Tyagi et al., 2013; Hu et al., 2021). Greyscale image is formed by considering the luminance (Y-component) for weighted RGB to YIQ conversion (I and Q produce chrominance and are ignored) (MathWorks, 2023a):

$$Y = 0.2989 * R + 0.5870 * G + 0.114 * B$$

In order to suppress the noise, greyscale image is first smoothed using low-pass kernel, such as average, median or gaussian, otherwise the differential nature of edge detection kernels (in successive stage) will amplify the noise. Gaussian smoothing is effective for edge detection purposes as it gives higher weightage to pixels near the edge, operates symmetrically and is computationally efficient. Once the smoothed image is obtained, it can be used for extracting useful features (in this case edges). Sobel, Prewitt and Canny edge detectors are a few techniques but the basic objective of edge detectors is to locate the edges at those points where gradient of *smoothed* input image is maximum with respect to some threshold. This threshold varies from technique to technique. These detectors have convolution kernels in both x- & y-directions for detecting horizontal and vertical edges (Ahmed, 2018). An example kernel for Sobel (S_x, S_y) and Prewitt (P_x, P_y) is given below in Equ. 1 with different coefficients of mask:

$$S_x = \begin{bmatrix} -1 & 0 & 1 \\ -2 & 0 & 2 \\ -1 & 0 & 1 \end{bmatrix}; S_y = \begin{bmatrix} 1 & 2 & 1 \\ 0 & 0 & 0 \\ -1 & -2 & -1 \end{bmatrix} \quad (1)$$

$$P_x = \begin{bmatrix} -1 & 0 & 1 \\ -1 & 0 & 1 \\ -1 & 0 & 1 \end{bmatrix}; P_y = \begin{bmatrix} -1 & -1 & -1 \\ 0 & 0 & 0 \\ 1 & 1 & 1 \end{bmatrix}$$

The magnitude & direction of edge is determined after convolution of mask with image pixels. Canny finds edges by employing a Gaussian smoothing filter and looking for local maxima of the gradient of smoothed image using Sobel filter approach. Canny introduces two thresholds to detect strong and weak edges, and is less sensitive to noise and more likely to detect true weak edges (connected to strong edges) (Ahmed, 2018; MathWorks, 2023b). In this work all three filters are applied on globally-binarized thermal images to study the level of details preserved/lost in each case.

In order to further improve the extracted edges or emphasize the black or white pixels, morphological operations are used (Wang et al., 2008). They are sliding window operations based on its shape or geometry; the window is called *structuring element* (see [25]). The value of each pixel in output image is based on the original image pixel values that appear in the geometry of sliding window (i.e.: neighborhood pixels). Choosing a *minimum* or *maximum* value among these neighboring pixels *erodes* or *dilates* the image (respectively). Performing these two operations in sequence give rise to *opening an image* (erosion followed by dilation) or *closing an image* (dilation followed by erosion).

Former one emphasizes the darker parts of image while performs *vice-versa*. These operations are useful when discontinuous, floating fragments of white/black pixels (in this case, ice edge/ background noise) appear after edge-preservation filtering.

2.2. Infrared ice-detection

Infrared thermography appears as a powerful remote sensing tool in studying icing physics (Karev et al., 2007; Karev and Farzaneh, 2003; Saylor et al., 2000). In the recent past Madi et al. (Madi et al., 2019) presented a succinct review of different ice mitigation techniques that can be integrated with IRT as an ice-detection approach for wind turbines. They conclude that IRT possesses promising applicability for all 5 mitigation methods (hot-air, heating filament & boots de-icing; microwave & ultrasonic anti-icing). However there's a need for further experimentation to assess their effectiveness and thermal efficiency (Madi et al., 2019). In another study, they investigated the diameter of single and a group of frozen water droplets using image processing on thermal images (Madi et al., 2021). This way they determined the volume occupied by these droplets while impacting on a hydrophilic surface. After performing experiments on cylindrical objects using IRT, they also propose that sequential thermal images can help track the build-up of ice on the leading edge, and similarly trace the deicing process if electro-thermal heating system is activated.

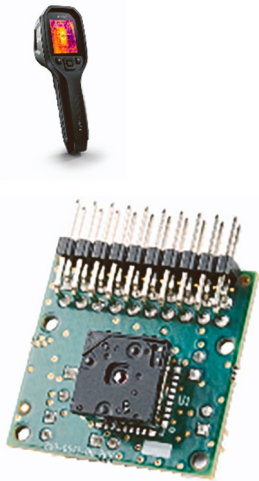

Similar work to detect ice accumulating on aircrafts has been done by Hao et al. (Hao et al., 2020) in which they use IRT to detect ice via heat signal generated by aircrafts' skin surface. They apply Principal Component Analysis (PCA) and Canny edge detection techniques as a part of thermal image processing, and evaluate EIDI as an ice mitigation system. Liu et al. (Liu et al., 2019) worked with Dielectric Barrier Discharge (DBD) plasma as an anti-icing/deicing technique for aircraft ice mitigation, and used FLIR® A615 thermal IR camera (with FLIR® IR window: IRW—4C) to map the resulting surface temperature distribution when plasma is actuated. They performed a comparative study between duty-cycled & continuous actuation modes of DBD plasma inside icing wind tunnel to study their efficiency. Continuing with the work, Kolbakir et al. (Kolbakir et al., 2020) used setup based on infrared thermography to analyze the performance of DBD plasma based anti-/de-icing actuators for glaze ice mitigation on aircrafts, and evaluated them on the basis of their geometry and width of exposed electrodes. Li et al. (Li et al., 2021) tried infrared thermography to detect ice defects inside aluminum honeycomb samples sandwiched by carbon-fibers. They also qualitatively compared three different photothermal excitation techniques in this regard. For quantitative analysis they determined the extent and location of ice accretion using adaptive Canny edge detection technique based on morphological filtering and Otsu algorithm. Veerakumar (Veerakumar, 2021) studied ice accretion on power lines using IRT and similar plasma based ice mitigation system.

Wang et al. (Wang et al., 2008) proposed two techniques to measure glaze & rime ice thickness on transmission lines and their insulators: wavelet transforms and floating threshold (for glaze icing on conductor and insulator) & optimal threshold and mathematical morphology (for conductors covered with rime ice of typically complicated shape and edges). The work is extended by Fazelpour et al. (Fazelpour et al., 2016) who studied icing on structures using both color & thermal imagery and applied similar floating-threshold based image processing techniques and morphological operations to both types of imagery. They conclude that information from both images is useful for detecting ice edge and ice thickness.

Muñoz et al. (Muñoz et al., 2016) carried out experiments on a section of wind turbine blade using thermal infrared radiometry. They evaluated different scenarios of no ice, thin ice, thick ice and partial ice covered regions on the white fiberglass turbine blade embedded with thermocouples. They also simulated the effect of surface dust accumulation on IRT measurements. Yousuf et al. (Yousuf et al., 2021) studied ice accretion on wind turbine blades using FLIR® A615 thermal infrared

Table 1

Salient features of low- and high-resolution thermal infrared cameras used for ice detection. FLIR TG-165 is supported by Lepton camera chip so the mass and price of chip are included.

Camera	Features	
	FLIR® TG-165 (supported by Lepton 80 × 60 resolution)	FLIR® T1030SC
		
Sensor	Uncooled VoX Microbolometer	FPA Uncooled Microbolometer
Framerate	8.6 Hz	30 Hz
NETD	< 50mK	< 20mK
Mass	0.9 g	1.9 kg – 2.1 kg
Cost	~ \$250	~ \$50,000

camera to analyze the effect of liquid water content, angle of attack, temperature and blades profile geometry on ice formation.

Riehm et al. (Riehm et al., 2012) used LWIR infrared thermometer to detect ice formation on roads due to wet road surface or ice crystals deposition. They conducted experiments both in the cold climate laboratory (on a piece of asphalt road with embedded Peltier element), as well as in field. Casselgren et al. (Casselgren et al., 2016) modifies the work to distinguish between dry, moist, wet, frosty, icy and snowy road surfaces using NIR camera system (FLIR® SC7100). They performed lab experiments on asphalt road pieces by illuminating the scene with three NIR wavelengths and replicated the disturbance from sun using a halogen lamp.

There have been some attempts to incorporate neural networks to predict ice accretion and ice thickness (Kreutz et al., 2019). Hao et al. (Hao et al., 2023) employed temperature elevation data obtained from thermal infrared imager to deduce ground ice thickness via back propagation neural networks. They collected 500 thermal images as a dataset from an experimental work. From these images 300 pixels from the icing area of each specimen were used to acquire useful features in order to train the network. These features were extracted from a theoretical model and 21st degree polynomial curve-fitting for comparison purpose. They report less than 10% error for the mentioned technique.

Literature review also suggests that it is possible to differentiate between fresh water and marine ice through IRT (Andleeb et al., 2020; Rashid et al., 2016a). Experiments were conducted by Rashid et al. (Rashid et al., 2016a) to determine the thermal conductivity and overall heat-transfer coefficients of freshwater and marine ice-blocks using FLIR® A310 IR camera. Then these values were used as input within the Multiphysics simulation tool with surrounding temperature as boundary conditions to create and verify temperature profiles. This study also suggests that IRT can be differentiated from freshwater ice using IRT (Rashid et al., 2015; Rashid et al., 2016b; Rashid et al., 2016c). Marine ice thickness is determined using active thermography by Rashid et al. (Rashid et al., 2019). They determined that the rate of change in the

surface temperature of ice, as measured from an LWIR camera, decreases with ice thickness. Moreover, it correlates with initial temperature of ice.

This sort of laboratory setup can be implemented in a real-time scenario by installing individually controlled heating elements underneath a large surface that will be monitored by an IR camera. For the purpose of locating ice, IR camera imagery can be obtained to perform image processing for segmenting ice from the scene image. The thickness of ice can be determined by the technique developed by Rashid et al. (Rashid et al., 2019), and proportional heating can be supplied to make the surface ice-free.

Such successful laboratory experimentation provides a lead to experiment IRT for offshore ice monitoring. However, the high cost of this setup for on-field monitoring is a major hurdle; IR camera itself being the most expensive and sensitive equipment. So, the idea behind this paper is to explore options to reduce the cost of a similar setup for outdoor cold environments: FLIR® manufactures a low cost, low resolution, on-chip camera. An experiment was designed to study if there is a possibility to detect ice, if an ice-detection system based on such a low-resolution camera is designed.

Section-2 of this paper elaborates on the experimental setup, section-3 presents the results obtained after image processing, and section-4 gives a conceptual overview of an economical, reliable ice detection and mitigation system followed by a concluding summary.

3. Design experiment

The experimental setup comprised a 13.5cm × 13.5cm × 10cm ice cube placed on a 785mm × 515mm coated Poly-Ethylene Terephthalate (PET) sheet by EBECO® (Fig. 2), a handheld, low-resolution (80 × 60) IR camera FLIR® TG-165 and a high-resolution (1024 × 768) IR camera FLIR® T1030SC. The sheet is heated by a powered heater (75 W, 230 V), and ice cube formed in an ordinary icebox or refrigerator. The reason for using PET sheet lies in its high emissivity value (approx. 0.85). Both the

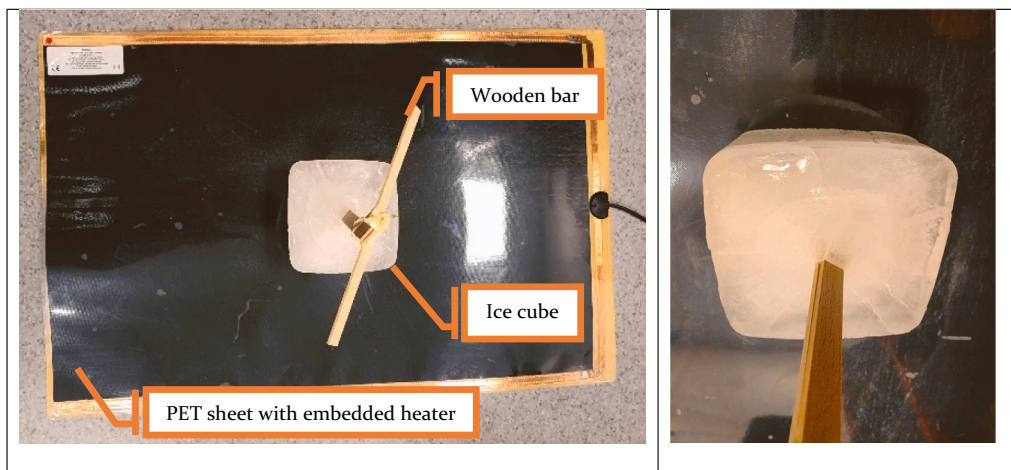


Fig. 2. Ice cube placed on PET sheet for infrared thermography analysis of low- and high-resolution images. Truecolor image of ice-block captured from above. The wooden bar was frozen with water to assist in moving the ice block later (rather than moving with hands) and hence prevent heat-loss. Thermal conductivity of wood is lesser than ice, so any residual thermal signature is avoided (Rashid et al., 2016a).

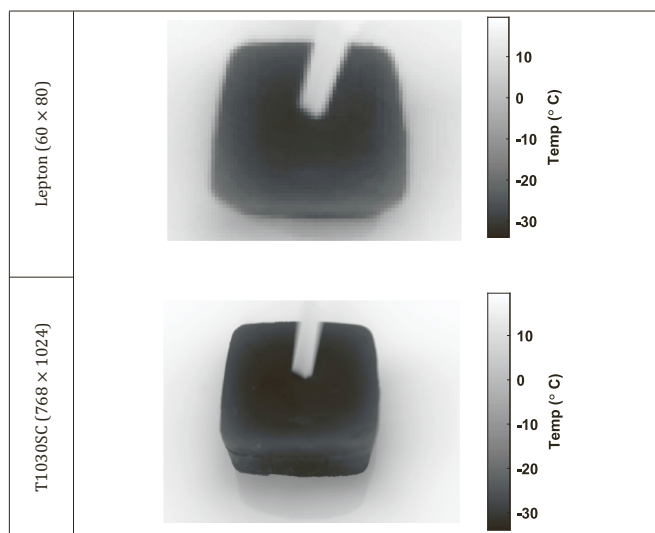


Fig. 4. Comparison of pixel information in greyscale view.

cameras feature uncooled microbolometers supporting LWIR; the low-resolution camera is 200 times less expensive than its counterpart; other salient characteristics are described below in Table 1. (See Fig. 1.) (See Fig. 3.)

The idea is to place the ice cube of known dimensions on a slightly heated PET sheet (to create temperature contrast for LWIR cameras). Images are captured with both high- and low-end cameras and snapped images are then processed using image processing techniques in MATLAB® to determine if both the cameras (especially low-resolution camera) can be used to segment ice for ice-detection purpose.

Since the handheld IR camera, TG-165 contains a low-resolution FLIR® Lepton chip (80 × 60 pixels), it is mentioned as Lepton in the coming text.

4. Results and discussion

Displays contour plots for visualizing temperature distribution in raw data. Owing to more pixel information captured by T1030SC and low value of thermal sensitivity (*i.e.*, NETD), it depicts narrow temperature changes. For instance, the temperature around the wooden bar is captured around $-32.7\text{ }^{\circ}\text{C}$, whereas that displayed by Lepton is in the

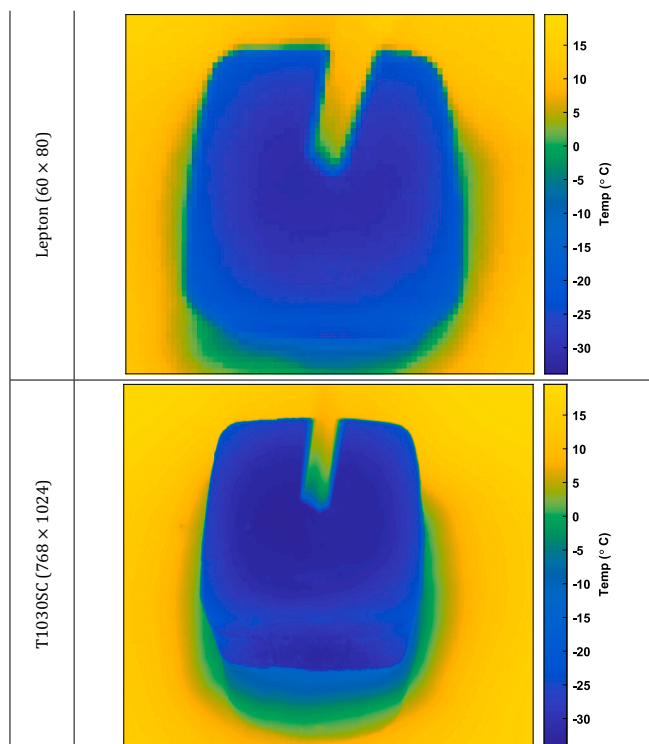


Fig. 5. Comparison of pixel information in colormap view.

range of $-28\text{ }^{\circ}\text{C}$ to $-30\text{ }^{\circ}\text{C}$.

Similarly, the greyscale and colormap view of the same images can help to visualize sharp boundary of the ice block in the case of T1030SC, which seems blurred in the Lepton camera image (see Figs. 4 & 5). A shadow of the ice block can be observed in these images along the x-axis (greenish appearance around the block in colormap), which is its reflection on the PET sheet. Thus the camera result gives a false reading of temperature in this zone, often referred as *reflected temperature*. Object (ice) is segmented in such a way to avoid the reflected temperature zone interfering with its detection.

When it comes to object detection, recognition, or image registration, corners and edges serve as important control point features. Fig. 6 presents Sobel, Prewitt, and Canny edge detection results for both the raw camera images: Canny comes out to be a good choice for both cases.

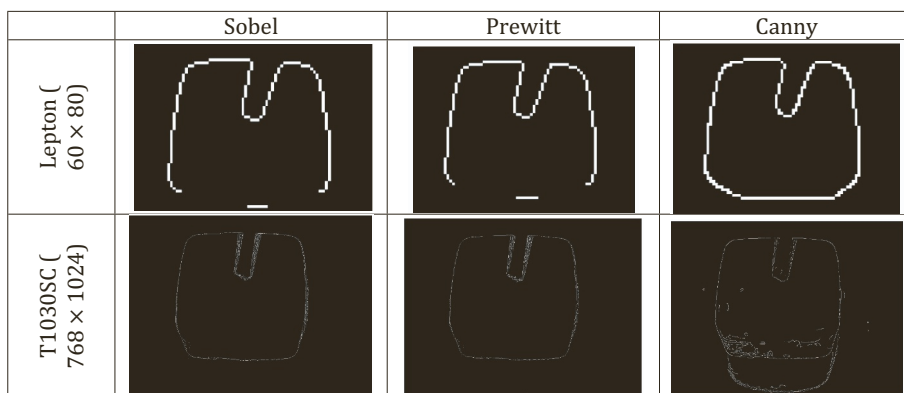


Fig. 6. Using different edge detection techniques on low- and high-resolution images.

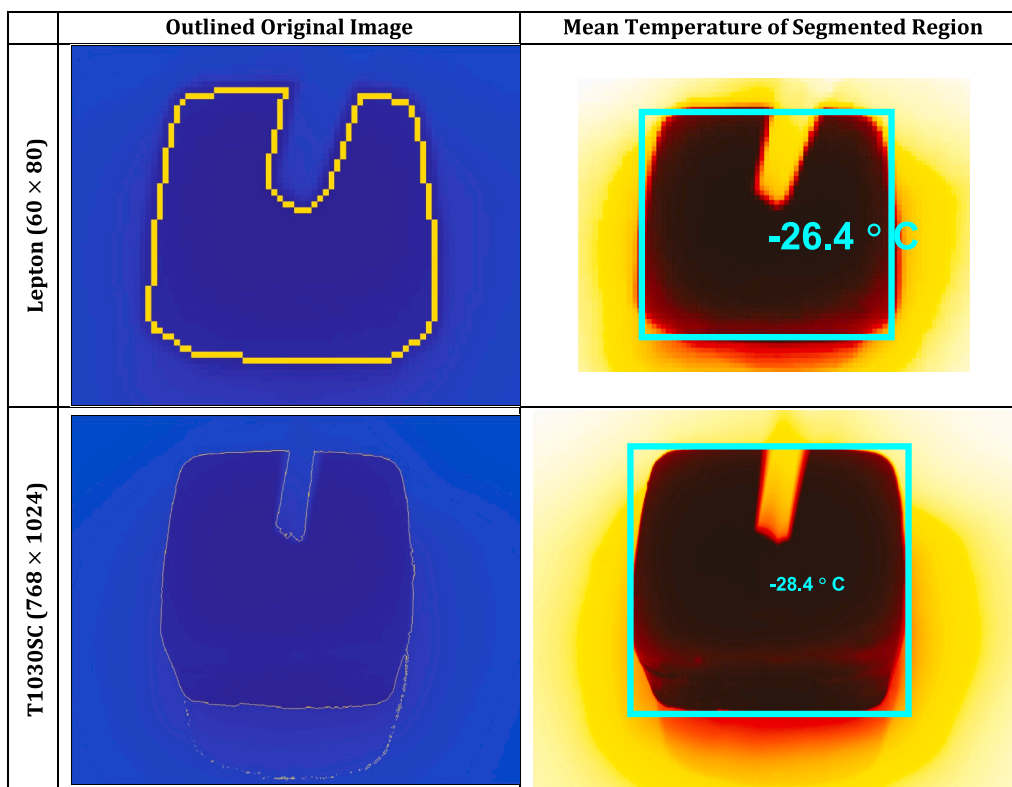


Fig. 7. Final results after applying morphological operations on thermal IR images.

However, since it is highly susceptible to strong and weak edges, it overestimates the geometry of ice by mistaking the object shadow (or reflected temperature). Overall, these binary gradient masks show the lines of high contrast but do not delineate the outline of the object of interest quite well: the gaps along the edges need to be eliminated.

For completely segmenting the images with clear boundaries and without noise, a closing morphological operation is applied to perform image dilation followed by image erosion. The process emphasizes the bright boundary obtained from binary gradient masking. Fig. 7 displays the final results of this process with a bounding box sketched around the detected ice with its average temperature. It was observed that both the cameras were able to capture and detect the ice after image processing. However, from the accuracy point of concern, FLIR® T1030SC camera is more accurate than the Lepton, which is why the difference of 2 °C in mean temperature is apparent.

For quantitative analysis, the boundary of the ice block was measured in pixels and compared with the real dimension. For Lepton

(80 × 60): $\frac{56\text{pixels}}{13.5\text{cm}} \approx 4\text{px.cm}^{-1}$ and for FLIR®T1030SC (1024 × 768): $\frac{609\text{pixels}}{13.5\text{cm}} \approx 45\text{px.cm}^{-1}$. It turns out that more pixels are available to define temperature distribution in the high-resolution camera.

5. Proof of concept

Based on the initial results validation obtained for ice detection through a low-end camera, an economical design for ice detection and mitigation system is proposed as shown below in Fig. 8. Arrowheads with numbering represent the sequence of operation. Ice accreted on target (for illustration here, in this case, a ship’s deck) shall be focused by FLIR® Lepton LWIR camera that will send acquired images to a controller. For future data storage and remote processing, the thermal images shall be uploaded to a cloud server, from where they will be downloaded by image processing software package such as Math-Works® to process them. Decisions about the presence/absence of ice

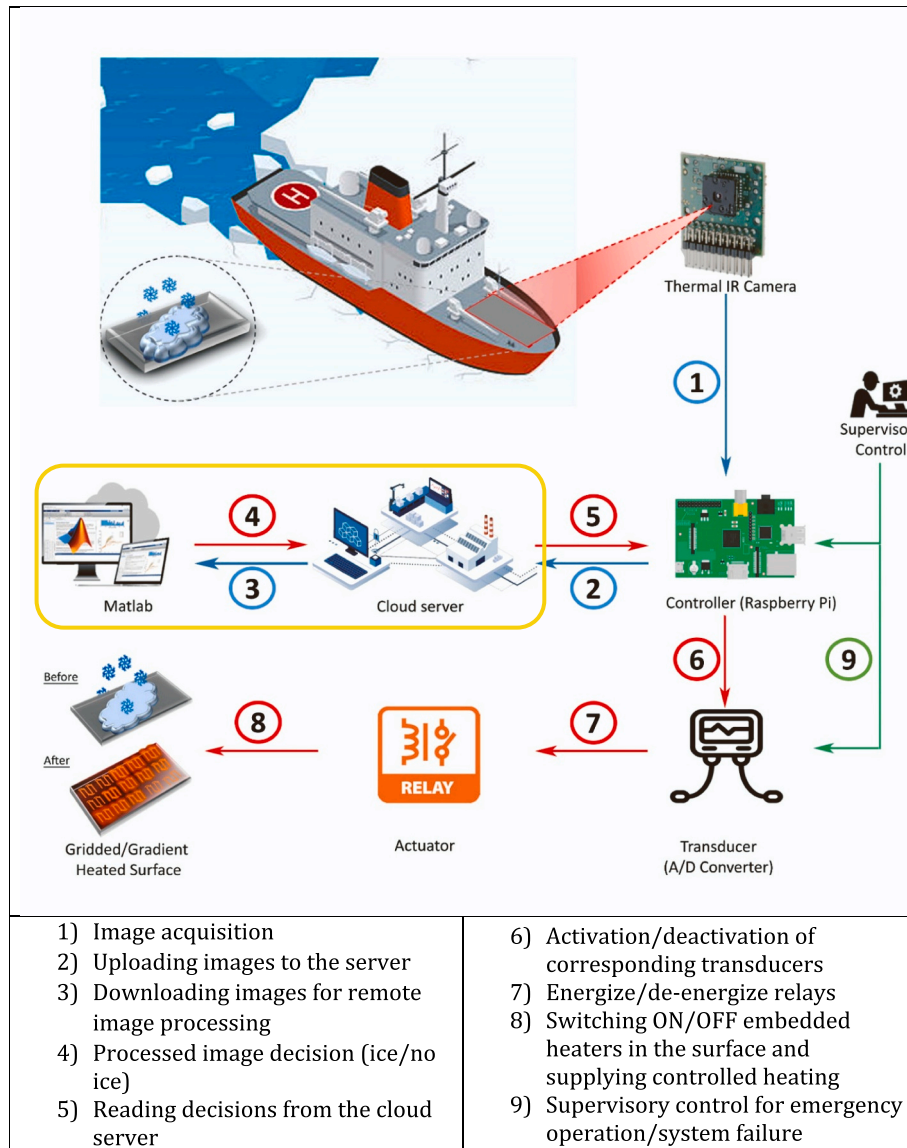


Fig. 8. Conceptual design of proposed ice detection and mitigation system.

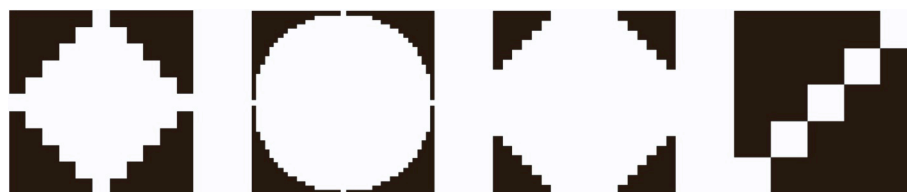


Fig. 1. Different structuring elements used for morphological operations: diamond, disc, octagon and slant line.

shall be communicated back to the controller that perceives the ice locations and in turn, energizes corresponding transducers/relays for heating at the ice accreted portion of the target surface. Remote ice detection through the server shall be only for research and development phase; in the future, the algorithm shall be run solely on the controller. To make the system more reliable and fail-safe, a supervisory control for emergency operation shall be added in which the whole surface can be heated/turned off.

A similar low-cost pixel heating platform has been developed for education and teaching purposes by Viola et al. (Viola et al., 2020; Rodriguez et al., 2021) that employs FLIR® Lepton thermal camera with

several heating elements. However, the system has not been yet tested for icing experiments. Through the development of conceptual ice-detection & mitigation system discussed in current paper (and pictured in Fig. 8), we aim for a cost-effective system that can be deployed directly in the field for icing studies.

6. Conclusion

Icing hazards can be mitigated by deploying the ice mitigation systems, for which ice detection is a preliminary step. Several direct and indirect ice detection techniques are used depending on the application.

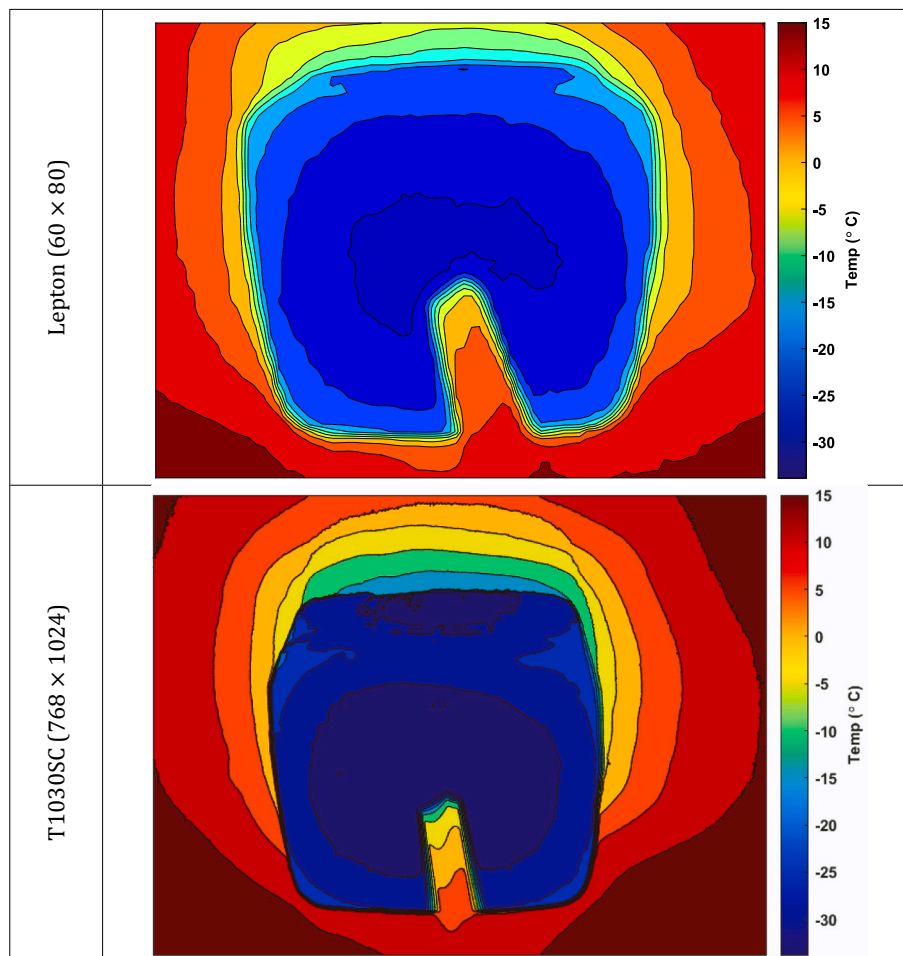


Fig. 3. Contour plot visualization for thermal infrared camera images.

Thermal infrared ice detection can be used as a non-contact, non-invasive technique with area scanning capability and can also be integrated with different ice-mitigation procedures. Though unfortunately, the heavy equipment cost of infrared thermography is a hurdle. This paper presented an idea of cost-effective solution to ice-detecting problems. To attain this purpose FLIR®'s low cost, lightweight, low resolution (80×60) thermal infrared camera is compared with a high resolution (1024×768). The results suggest the interplay of resolution, accuracy, and cost; since more pixels are available in a high-end FLIR® T1030SC IR camera to store thermal information, a sharp and accurate image is obtained in contrast to FLIR® Lepton. Similarly, the quantitative analysis concludes where 45 pixels/cm are available to cover the scene for a high-resolution camera, only 4 pixels/cm capture the scene temperature. Nevertheless, these smaller pixels are still sufficient to detect ice and fulfil the goal.

CRedit authorship contribution statement

Adeel Yousif: Methodology, Software, Writing – original draft, Writing – review & editing. **Hassan Khawaja:** Methodology, Supervision. **Muhammad S. Virk:** Supervision.

Declaration of Competing Interest

The authors declare the following financial interests/personal relationships which may be considered as potential competing interests:

Adeel Yousif reports financial support was provided by Research Council of Norway.

Data availability

Data will be made available on request.

Acknowledgement

The work reported in this paper is supported by nICE project (Project # 324156) funded by UiT & Research Council of Norway.

References

- Ahmed, A.S., Oct 15 2018. Comparative study among Sobel, Prewitt and Canny edge detection operators used in image processing. *J. Theor. Appl. Inf. Technol.* 96 (19) [Online]. Available: <http://www.jatit.org/volumes/Vol96No19/20Vol96No19.pdf>.
- Andleeb, Z., et al., 2020. Multiphysics study of infrared Thermography (IRT) applications (in English). *Int. J. Multiphys.* 14 (3), 249–271. <https://doi.org/10.21152/1750-9548.14.3.249>.
- Cao, Y., Chen, K., Feb 03 2016. Helicopter icing. *Aeronaut. J.* 114 (1152), 83–90. <https://doi.org/10.1017/S0001924000003559>.
- Casselgren, J., Rosendahl, S., Sjödaahl, M., Jonsson, P., Feb 2016. Road condition analysis using NIR illumination and compensating for surrounding light. *Opt. Lasers Eng.* 77 <https://doi.org/10.1016/j.optlaseng.2015.08.002>.
- Farzaneh, M., 2013. Insulator icing flashover. In: Presented at the 2013 Annual Report Conference on Electrical Insulation and Dielectric Phenomena [Online]. Available: <https://ieeexplore.ieee.org/document/6748324>.
- Farzaneh, M., Kiernic, J., 1995. Flashover problems caused by ice build-up on insulators. *IEEE Electr. Insul. Mag.* Available: <https://ieeexplore.ieee.org/document/372510>.
- Farzaneh, M., Melo, O.T., Dec 1990. "Properties and effect of Freezing rain and Winter fog on Outline Insulators," (in English). *Cold Reg. Sci. Technol.* 19 (1), 33–46. [https://doi.org/10.1016/0165-232x\(90\)90016-P](https://doi.org/10.1016/0165-232x(90)90016-P).
- Fazelpour, A., Dehghani, S.R., Masek, V., Muzychka, Y.S., Oct, 2016. Infrared image analysis for estimation of ice load on structures. In: Presented at the Arctic Technology Conference. St. John's, Newfoundland and Labrador, Canada [Online].

- Available: <https://onepetro.org/OTCARCTIC/proceedings/16OARC/All-16OARC/OTC-27409-MS/84797>.
- Hansen, E.S., 2012. Numerical modelling of marine icing on offshore structures and vessels. In: Master of Science in Physics and Mathematics, Department of Physics. Norwegian University of Science and Technology [Online]. Available: https://ntn.uopen.ntnu.no/ntnu-xmlui/bitstream/handle/11250/246746/566253_FULLTEXT01.pdf.
- Hao, L., Li, Q., Pan, W., Li, B., Jun 27 2020. Icing detection and evaluation of the electro-impulse de-icing system based on infrared images processing (in English). *Infrared Phys. Technol.* 109. <https://doi.org/10.1016/j.infrared.2020.103424>.
- Hao, L., Li, Q.Y., Pan, W.C., Yao, R., Liu, S.Y., Feb 2023. Ice accretion thickness prediction using flash infrared thermal imaging and BP neural networks (in English). *IET Image Process.* 17 (3), 649–659. <https://doi.org/10.1049/ipr2.12662>.
- Hu, Q., Yuan, W., Shu, L.C., Jiang, X.L., Wang, S.J., 2014. Effects of electric field distribution on icing and flashover performance of 220kV composite insulators (in English). *IEEE T Dielect El In* 21 (5), 2181–2189. <https://doi.org/10.1109/Tdie.2014.002181>.
- Hu, Q., et al., 2021. A method for measuring ice thickness of wind turbine blades based on edge detection. *Cold Reg. Sci. Technol.* 192 (103398) <https://doi.org/10.1016/j.coldregions.2021.103398>.
- Jin, J.Y., Virk, M.S., 2019. Seasonal weather effects on wind power production in cold regions— a case study. *Intern. J. Smart Grid CleanEnergy* 8 (1). <https://doi.org/10.12720/sgce.8.1.31-37>.
- Kandelin, N., 2021. Icing factors affecting railway traffic. In: Masters in Material Science, Faculty of Engineering Sciences. Tampere University, Finland [Online]. Available: <https://trepo.tuni.fi/bitstream/handle/10024/134740/KandelinNiklas.pdf>.
- Karev, A.R., Farzaneh, M., May 25, 2003. Infrared laboratory measurement of ice surface temperatures during experimental studies on the formation of ice accretions. In: Presented at the Thirteenth International Offshore and Polar Engineering Conference, Honolulu, Hawaii, USA [Online]. Available: <https://onepetro.org/ISOPEIOPEC/proceedings/ISOPE03/All-ISOPE03/ISOPE-I-03-058/8327>.
- Karev, A.R., Farzaneh, M., Kollár, L.E., 2007. Measuring temperature of the ice surface during its formation by using infrared instrumentation. *Int. J. Heat Mass Transf.* 50 (3–4), 566–579. <https://doi.org/10.1016/j.ijheatmasstransfer.2006.07.015>.
- Kolbakir, C., Hu, H., Liu, Y., Hu, H., Dec 2020. An experimental study on different plasma actuator layouts for aircraft icing mitigation (in English). *Aerosp. Sci. Technol.* 107 (106325). <https://doi.org/10.1016/j.ast.2020.106325>.
- Kreutz, M., et al., 2019. Machine learning-based icing prediction on wind turbines (in English). In: 52nd CIRP Conference on Manufacturing Systems (CMS), vol. 81, pp. 423–428. <https://doi.org/10.1016/j.procir.2019.03.073>.
- Li, Q., Li, B., Xu, H., Bai, T., Jun 8 2021. Infrared thermal detection of ice defects inside honeycomb sandwich skin. *IEEE Instrument. Measure. Magaz.* 24 (4), 59–64. <https://doi.org/10.1109/MIM.2021.9448253>.
- Liu, Y., Kolbakir, C., Hu, H.Y., Meng, X.S., Hu, H., Jun 2019. "an experimental study on the thermal effects of duty-cycled plasma actuation pertinent to aircraft icing mitigation," (in English). *Int. J. Heat Mass Transf.* 136, 864–876. <https://doi.org/10.1016/j.ijheatmasstransfer.2019.03.068>.
- E. Madi, K. Pope, W. M. Huang, and T. Iqbal, "A review of integrating ice detection and mitigation for wind turbine blades," (in English), *Renew. Sust. Energ. Rev.*, vol. 103, pp. 269–281, Apr 2019, doi: <https://doi.org/10.1016/j.rser.2018.12.019>.
- Madi, E., Pope, K., Huang, W., 2021. Estimating the volume of frozen water droplets on a cold surface during the phase change with thermal image processing. *Measurement* 183 (109907). <https://doi.org/10.1016/j.measurement.2021.109907>.
- MathWorks, 2023a. Convert RGB Color Values to NTSC Color Space. MathWorks. <https://www.mathworks.com/help/images/ref/rgb2ntsc.html> (accessed Mar 02, 2023).
- MathWorks, 2023b. Find edges in 2-D grayscale Image. MathWorks. <https://www.mathworks.com/help/images/ref/edge.html> (accessed Feb 28, 2023).
- Muhammed, M., Virk, M.S., Mar 28 2022. Ice accretion on fixed-wing unmanned aerial Vehicle—A review study. *Drones* 6 (4). <https://doi.org/10.3390/drones6040086>.
- Muhammed, M., Virk, M.S., 2023a. Steady and Time Dependent Study of Laminar Separation Bubble (LSB) behavior along UAV Airfoil RG-15. *Intern. J. Multiphys.* [Online]. Available: <http://journal.multiphysics.org/index.php/IJM/article/view/853>.
- Muhammed, M., Virk, M.S., 2023b. Ice accretion on rotary-wing unmanned aerial vehicles—a review study. *Aerospace* 10 (3). <https://doi.org/10.3390/aerospace10030261>.
- Muñoz, C.Q.G., Márquez, F.P.G., Tomás, J.M.S., Nov 2016. Ice detection using thermal infrared radiometry on wind turbine blades (in English). *Measurement* 93, 157–163. <https://doi.org/10.1016/j.measurement.2016.06.064>.
- Mustafa, M.Y., Virk, M.S., 2011. Atmospheric ice detection and measurement using image processing based techniques in the visible and infrared spectrums. *Multiphysics* [Online]. Available: <https://static1.squarespace.com/static/5c9f89c101232cd41297d67/t/5d7943181dbec613b38a1d48/1568228126428/MULTIPHYSICS+2011+++Abstracts.pdf>.
- Network Rail. Why can't normal train services run on snow and ice? [Online]. Available: <https://www.networkrail.co.uk/stories/why-cant-normal-train-services-run-on-snow-and-ice/>.
- Qi, Z., et al., July 04 2022. Effects of static icing on flashover characteristics of high-speed train roof insulators. *Coatings* 12 (7). <https://doi.org/10.3390/coatings12070950>.
- Rashid, T., Khawaja, H., Edvardsen, K., Mughal, U.N., 2015. Infrared thermal signature evaluation of a pure Ice Block. In: Presented at the SENSORCOMM 2015: The Ninth International Conference on Sensor Technologies and Applications, Venice, Italy [Online]. Available: <https://munin.uit.no/bitstream/handle/10037/8942/article.pdf>.
- Rashid, T., Khawaja, H.A., Edvardsen, K., 2016b. Ice Detection Experimentation Setup using infrared and active heating. In: Presented at the SENSORCOMM 2016: The 10th International Conference on Sensor Technologies and Applications, Niece, France [Online]. Available: <https://munin.uit.no/handle/10037/12044?show=full>.
- Rashid, T., Khawaja, H.A., Edvardsen, K., 2016c. Ice detection of pure and saline ice using infrared signature. *Sens. Transd.* 206 (11), 82–87 [Online]. Available: <https://munin.uit.no/handle/10037/10208>.
- Rashid, T., Khawaja, H.A., Edvardsen, K., 2019. "measuring thickness of marine ice using IR thermography," (in English). *Cold Reg. Sci. Technol.* 158, 221–229. <https://doi.org/10.1016/j.coldregions.2018.08.025>.
- Rashid, T.K., Abbas, Hassan, Edvardsen, Kåre, 2016a. Determination of thermal Properties of fresh water and sea water ice using multiphysics analysis. *Int. J. Multiphys.* 10 (3), 277–290. <https://doi.org/10.21152/1750-9548.10.3.277>.
- Riehm, M., Gustavsson, T., Bogren, J., Jansson, P.E., Dec 2012. Ice formation detection on road surfaces using infrared thermometry (in English). *Cold Reg. Sci. Technol.* 83–84, 71–76. <https://doi.org/10.1016/j.coldregions.2012.06.004>.
- Rodriguez, C., Viola, J., Chen, Y., 2021. Data-driven modelling for a high order multivariable thermal system and control. *IFAC-PapersOnLine* 54 (20), 753–758. <https://doi.org/10.1016/j.ifacol.2021.11.262>.
- Ryerson, C.C., Jan 2011. Ice protection of offshore platforms (in English). *Cold Reg. Sci. Technol.* 65 (1), 97–110. <https://doi.org/10.1016/j.coldregions.2010.02.006>.
- Saylor, J.R., Smith, G.B., Flack, K.A., 2000. Infrared imaging of the surface temperature field of water during film spreading. *Phys. Fluid* 12 (3), 597–602. <https://doi.org/10.1063/1.870265>.
- Szilder, K., Yuan, W., Jun 20 2017. In-flight icing on unmanned aerial vehicle and its aerodynamic penalties. *Prog. Flight Phys.* 9, 173–188. <https://doi.org/10.1051/eucass/2016090173>.
- Tyagi, S., Ambia, H., Tyagi, S., 2013. Comparative study of image enhancement and analysis of thermal images using image processing and wavelet techniques. *Intern. J. Comput. Eng. Res.* 3 (4) [Online]. Available: <https://citeseerx.ist.psu.edu/document?repid=rep1&type=pdf&doi=a0493e1d4d1aa03200ac8fc4a1942ff80eeb1f75>.
- Veerakumar, R., 2021. An Experimental Study of Icing Physics and Anti/de-Icing Techniques for Structural Cables. *Aerospace Engineering*, Iowa State University [Online]. Available: <https://dr.lib.iastate.edu/entities/publication/be2f6f2d-ded0-4c2d-9cba-7850016036d6>.
- Viola, J., Rodriguez, C., Chen, Y., 2020. PHELP: Pixel heating experiment learning platform for education and research on IAI-based smart control engineering. In: Presented at the 2nd International Conference on Industrial Artificial Intelligence (IAI), Shenyang, China [Online]. Available: <https://ieeexplore.ieee.org/stamp/stamp.jsp?arnumber=9262160>.
- Virk, M.S., Afzal, F., 2018. Review of Icing Effects on Wind Turbine in Cold Regions. In: Presented at the The International Conference on Electrical Engineering and Green Energy (CEEGE 2018) [Online]. Available: https://www.e3s-conferences.org/articles/e3sconf/abs/2018/47/e3sconf_eege2018_01007/e3sconf_eege2018_01007.html.
- Virk, M.S., Mustafa, M.Y., Al-Hamdan, Q., 2011. Atmospheric ice accretion measurement techniques. *Int. J. Multiphys.* 5 (3) [Online]. Available: <https://munin.uit.no/bitstream/handle/10037/25710/article.pdf>.
- Wang, X., Hu, J., Wu, B., Du, L., Sun, C., 2008. Study on edge extraction methods for image-based icing on-line monitoring on overhead transmission lines. In: 2008 International Conference on High Voltage Engineering and Application, Chongqing, China. IEEE, pp. 661–665. <https://doi.org/10.1109/ICHVE.2008.4774022> [Online]. Available: <https://ieeexplore.ieee.org/document/4774022>.
- Wei, K.X., Yang, Y., Zuo, H.Y., Zhong, D.Q., December 23 2019. A review on ice detection technology and ice elimination technology for wind turbine (in English). *Wind Energy* 23 (3), 433–457. <https://doi.org/10.1002/we.2427>.
- Yousif, A., Jin, J.Y., Sokolov, P., Virk, M.S., Aug 2021. Study of ice accretion on wind turbine blade profiles using thermal infrared imaging (in English). *Wind Eng.* 45 (4), 872–883. <https://doi.org/10.1177/0309524x20933948>.